Horizontal directional drilling (HDD) alignment optimization using ant colony optimization

Fernando Patino-Ramirez,[1,2], Carrie Layhee[2], Chloé Arson[1]*

[1] School of Civil and environmental engineering, Georgia Institute of Technology, Atlanta, GA, USA.

[2] Haley Aldrich Inc, USA.

Abstract

Horizontal Directional Drilling (HDD) is a trenchless method that consists in drilling an inclined and curved bore from an entry point to an exit point. In practice, HDD is designed iteratively by trial and error, to minimize the cost under geometric and mechanical constraints. In this paper, we optimize the drill path with continuous implementations of an Ant Colony Optimization (ACO) algorithm that sets the depth of the alignment and its entry and exit angles as the design parameters to optimize, to ensure minimal drill path length (cost), avoid collapse or instability (mechanical constraints) and remain in the construction domain (geometric constraint). We compare the ACO results to the drill paths designed in practice in two different scenarios: one in which the entry and exit points are fixed, and one in which the geometry of the central segment is constrained. Results show that ACO can be used to automate the otherwise time-consuming design process while minimizing the drill path length and the costs associated to it.

Keywords: Horizontal Directional Drilling (HDD), Ant Colony Optimization (ACO), performance, mechanical integrity, stability, trenchless

1. Introduction

Horizontal directional drilling (HDD) is used to drill cavities through geomaterials at relatively shallow depths. The basic sequence of steps of an HDD installation consists in a preliminary design, followed by the drilling of a pilot bore from the drilling rig (entry point) to the exit point following the geometry of the designed path. Then, the pilot hole is reamed, i.e., it is sequentially enlarged by changing the drilling head used for the pilot bore with a reamer, which concentrically increases the cavity along the pilot alignment. Finally, the pullback step consists in the installation of the product or casing pipe, which is pulled through the reamed borehole, usually from the exit point towards the entry.

Compared to conventional cut and cover (1,2), HDD presents advantages in cost, environmental impact, land use and project timeline. HDD is also advantageous compared to other trenchless methods. For instance, HDD is usually less expensive than micro-tunneling (MT), despite the fact that HDD alignments are typically longer than MT alignments. This is because HDD is done with less specialized equipment and does not require entry/exit shafts to reach the drill depth. While auger drills are easily infiltrated by pore water under high groundwater tables, HDD performs well under high porewater pressure. Additionally, the jacking loads and torsional stresses on the auger flight usually limit the maximum drill length of auger borings (1–3). HDD is exempt of that limitation.

Since its first implementation in 1971 in a natural gas installation crossing the Pajaro river in Watsonville California (4), HDD has been successfully adapted to complex geological conditions and geometrical constraints. To date, the longest installation with a single drill rig crossed the Qin river in Jiaozuo, Henan province in China with a total drill path length of 1.75km. Installations with two drill rigs achieved a maximum drill length of 3.3km -- for example, the gas pipeline installation across the Yangtze river in China (4).

Despite its increasing popularity in the engineering practice (2), many fundamental mechanisms pertaining to the design of HDD remain unknown. Current research aims to increase the alignment and maximize the cost efficiency of HDD (5–7). Mechanical

evaluations of HDD focus either on borehole instability or on pipe integrity (2). By contrast, no method exists to optimize the drill path, which is still determined iteratively to this date: an initial estimation of the alignment is tested and gradually adjusted until a path that complies with the design criteria has been found (3). To overcome this limitation, we explain and test a numerical method that sequentially calculates the alignment of the drill path to satisfy mechanical design constraints (here, borehole stability and pipe integrity) while minimizing the installation cost (here, the total drill length). Section 2 describes the design process of HDD alignments. We first present a design method based on geometrical constraints (e.g., constructability angles, segment lengths and depth of cover from the ground surface and obstacles inside the soil). Then we explain a design method based on mechanical considerations (i.e., borehole stability and pipe integrity). Section 3 summarizes the general framework of Ant Colony Optimization (ACO) and explains the current implementation of ACO applied to the specific problem of HDD alignment design (ACO-HDD). The ACO-HDD method is tested for two design scenarios in Section 4. Section 5 presents the conclusions of this study.

2. HDD alignment design

Approximate locations for the entry and exit points of the drilling path are decided after completing a preliminary study that also assesses the relevance of HDD for the project at stake. Then the geometry of the HDD is designed to fit the drill path within the assigned domain. The mechanical design is the last step, to test borehole stability and pipe integrity during the whole construction. If the initial design does not comply with the assigned constraints, it is iteratively adjusted.

2.1 Geometric design

The geometric alignment considered in this paper consists of at least 5 segments, starting with an entry tangent from the rig side, followed by a curved segment that reaches the central portion of the alignment. This central portion consists of at least one

straight segment, but more complex alignments may include extra straight and curved portions (with vertical, horizontal or compound curvature). The central portion is typically designed first, followed by adjacent segments and the exit tangent. The radius of curvature of the curved segments is chosen so as to prevent excessive bending stresses as the pipe is pulled back from the surface through the curved segments, and thus depends on the material properties and diameter of the pipe. In this study, the radius of curvature is fixed. Therefore, once the entry/exit angles of the vertical projection of the curve are set (from the end points of the adjacent segments), the vertical projection of the curve (Δy in Figure 1) is fully determined. In the following, we use the terms "vertical curve" and "vertical projection of the curve" interchangeably.

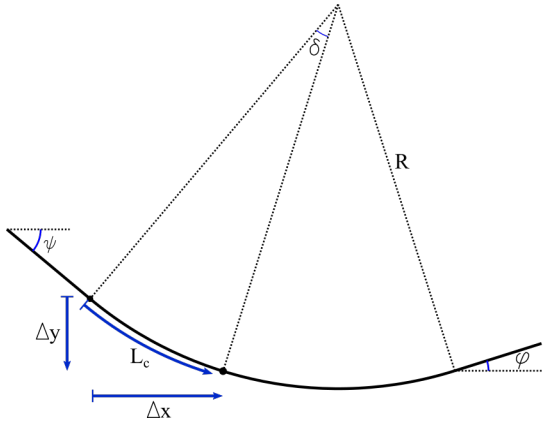

Figure 1. Diagram showing the vertical projection of the HDD curve diagram, with parametrization along the x direction

The parametrization of the horizontal projection of the curve (Δx in Figure 1) as a function of the stationing of the project is found according to Eq 1-4 below:

$$S = sign(\varphi - \psi) \tag{1}$$

$$\delta = \sin^{-1}\left(\sin\psi + S\left({}^{\Delta x}/_{R}\right)\right) \tag{2}$$

$$\Delta y = S \cdot R(\cos\psi - \cos\delta) \tag{3}$$

$$L_c = R \cdot \delta \tag{4}$$

Good practices recommend the inclusion of straight segments of a certain minimum length preceding and following curves for constructability. Figure 2 shows an example

of an HDD geometric alignment in plan view (top view, plane XY) and in profile view, i.e. following the direction of the stationing of the alignment in the horizontal axis and the elevation in the vertical axis.

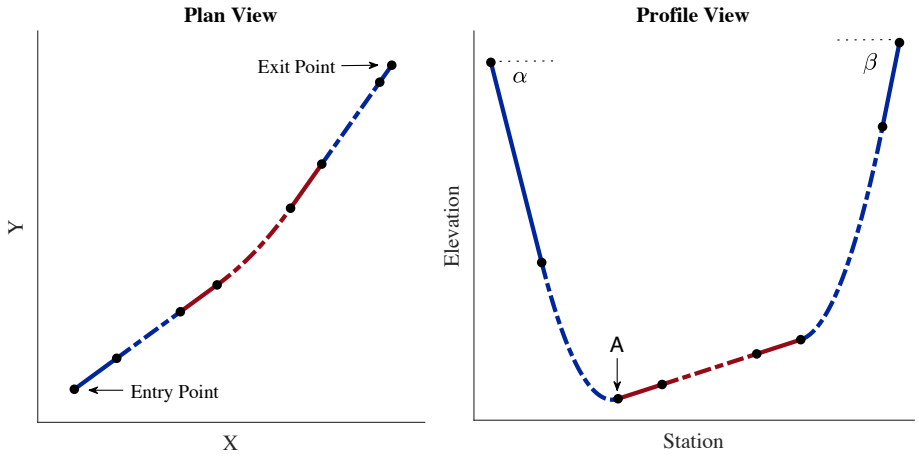

Figure 2. Example of a typical HDD alignment. Left: Plan (top, XY plane) view Right: Profile (Stationing vs Elevation) view. Solid lines correspond to straight segments while dashed lines correspond to curves. Central portion of the alignment highlighted in red.

The alignment design is optimized by adjusting three parameters: the elevation H of point A in the central portion of the alignment, the entry angle (α) and the exit angle (β) which control the entry and exit tangents and their neighboring vertical curves. The range of variation of α and β is constrained by constructability limitations and is usually between of 5 and 18 degrees. We adopt the convention that the drill progresses from the rig side, located on the left side of the diagrams, to the exit side located on the right; angles are measured in reference to the horizontal line and are counted positive when going counter-clockwise – therefore, α and β are positive and negative respectively.

A geometrically viable alignment is such that: (i) It can still fit within the fixed bounds of the HDD drill. (ii) It yields a minimum depth of cover along the alignment that is at least equal to the minimum allowable, in order to prevent surface disturbance

and damage to the product pipe. Usually the minimum depth is between 5 and 15ft, depending on the application, soil/rock conditions, surrounding foundations and existing utility networks. (iii) The length of every straight segment is at least equal to the minimum defined for constructability. This minimum usually corresponds to one to three times the length of the drilling rods used for drilling; in some cases, this minimum can be set to zero, creating alignments with no transition between curves.

Lastly, the parameter H varies in a range that depends on the other geometric parameters. The minimum value of H, i.e. the lowest possible elevation of point A, and therefore the deepest drill path, is obtained by setting the entry and exit angles to their maximum magnitude and setting the entry and exit points as far away from each other as possible. Conversely, the maximum value of H is the shallowest path that still complies with the depth of cover constraints. Once the geometrical constraints have been cleared, the mechanical viability of the given alignment is tested.

2.2 Mechanical Design

Borehole Stability

The drilling fluid plays a fundamental role in every step of the HDD process: pilot drilling, reaming and pullback. The continuous flow of drilling mud cools down the drill head and the reamers, transports the cuttings to the exit pit for effective drilling and reaming, provides lubrication for the tooling and product pipe inside the borehole, seals fractures and high permeability paths that can lead to inadvertent returns to surrounding formations, improves the stability of the cavity and thus prevents collapse (8–11).

The drilling fluid is a non-Newtonian fluid, usually made from a mix of water, bentonite and extra additives. An external pump circulates the fluid from outside the borehole through the drilling rods and flows back to the free surface through the annular space between the drill rods and the borehole or between the product pipe and the

borehole (during pullback) following the path of least resistance. The minimum drilling pressure (MDP) necessary to induce recirculation of the drilling mud (21) is equal to the sum of the difference of pressure head between the pumping station and the drill path and of the fluidic drag developed in the annular space (controlled by the suspended cuttings and by the viscosity and yield point of the fluid).

The injection of the pressurized drilling fluid induces a deformation of the borehole. This phenomenon was modeled using the theory of cylindrical cavity expansion under different scenarios (5,9,12). The so-called Delft equation (12) assumes that the far field stress around the cavity is isotropic, and that the cavity wall and the elasto-plastic boundary are circular. It is assumed that cavity shear failure, known as blowout, occurs as the internal pressure reaches the limit pressure of the cavity, causing large radial displacements and plastic expansion. The Queen's equation (5) releases the assumption of isotropic far field stresses, considering biaxial stresses, but still assumes a circular elasto-plastic boundary around the region. The formulation assumes that shear failure develops either at the top (crown) or at the side of the cavity, simplifying the analysis. The development of more accurate analytical solutions to this problem remains an active field of research to this day. Despite its simplifying assumptions, the Delft equation remains the most commonly accepted formulation and will therefore be adopted in the present study to find the maximum allowable pressure (MAP) of the drilling fluid before blowout is triggered.

Product pipe Integrity

The second step of the mechanical analysis aims to calculate the stresses (and subsequent strains) in the pipe as it is pulled back from the exit to the entry point of the drill alignment. External loads on the product pipe are:

1. The tensile force due to the pull operation from the rig. The required force to pull the pipe is a function of: the weight component of the pipe in the pull direction, the friction from the contact between the pipe and the

borehole and/or the ground surface, the fluidic drag arising from the shear resistance of the viscous drilling fluid around the pipe and the extra frictional stresses due to increased contact forces on the pipe as the pipe is bent around curved segments.

2. The bending moment applied as the pipe is pulled through curves. Bending induces extra tensile stress in the outermost fibers of the pipe, therefore the critical stress condition must consider the combined tensile stress from tension and bending of the pipe. Depending on the material that makes the pipe, the way to calculate stresses due to bending varies; ductile iron pipes usually include flexible joints which dissipate the bending stress around curves, while steel pipes behave as rigid beams when bent around curves; the resulting increase in friction from the contact is calculated as described in (5,13). Lastly, plastic pipes (HDPE or FPVC) are usually considered flexible and thus the increase in tensile forces is modeled using the capstan effect (14).

In addition to testing the pipe for tensile failure, it is necessary to check that the pipe remains stable, i.e., that it does not buckle. In order to avoid excessive friction between the pipe and the borehole and thus decrease the MDP, the borehole is usually considerably larger than the product pipe. Therefore, the pipe rests inside the borehole under unconstrained conditions sustaining the pressure head from the column of drilling fluid and possibly some earth loading. Buckling calculations are thus intended to prevent possible collapse or excessive oval deformation, which may alter the installation of conduits inside the product pipe (3).

Once the individual mechanisms affecting the integrity of the pipe are quantified, the deformation of the product pipe under the combination of loads is compared to the maximum recommended deflection and the pipe stress is compared to the pipe material strength parameters. Factors of safety depend on the pipe material and manufacture (3).

3. Ant Colony Optimization (ACO)

3.1 Background and literature review

Physical studies have shown the outstanding capabilities of ants to forage complex domains without any means of direct communication between them (15). Ant colonies display a very effective swarm behavior based on the deposition of a chemical substance, which allows the whole colony to sequentially find the most efficient way to exploit the resources of a domain. Inspired by this behavior, several authors created ant-inspired computational optimization algorithms, which were then grouped into a general framework known as Ant Colony Optimization (ACO). ACO is a family of meta-heuristic algorithms that solve complex combinatorial problems (16) by using a computational swarm intelligence, where individual entities contribute to the global, collective exploration knowledge of the domain, sequentially improving the solutions to the tested problem, to converge to an optimal.

The common framework for ant inspired optimization was initially proposed for solving discrete combinatorial optimization problems and was applied to the common benchmark traveling salesman problem (12). Other early applications of ACO include routing in communication networks, quadratic assignment problems and job-scheduling (17). Since the initial algorithms proposed in the early 90's, the capabilities and applications of ACO have advanced significantly, being now recognized as an effective and flexible technique with a vast number of different implementations suitable for virtually any optimization conditions. Comprehensive reviews were presented in (16,18)

Applications specific to civil engineering have focused mainly on transportation, for traffic routing more so than infrastructure design, for example for train traffic and bus network design (19,20). In this study we make use of ACO to find the optimal combination of geometric parameters that minimizes the total length of the HDD drilling path. We use the ACO implementation described in (21), which can be used for

mixed variable problems, including discrete (ordinal and categorical) and continuous variables. In the case studies presented below, we only use continuous variables. The implementation can be improved to include discrete variables, using the same base algorithm.

3.2 Algorithm principle

The basic principle of the algorithm is inspired by the foraging strategies employed by an ant colony that is inside a complex maze with numerous multiply-connected paths. Initially, the colony has no prior knowledge of the domain. Therefore, at first, individual ants explore the maze randomly. Each exploration yields a certain path. At the end of a given path, the ant may find a food source. A score is assigned to each path, in proportion to the quality and amount of the food source associated with the path. This score can be understood as a concentration of pheromone. This pheromone is deposited along the path in a process known as stigmergy, which is an indirect form of communication between ants based on a modification of the environment, which becomes the collective knowledge and memory of the colony (22).

The scores assigned to paths explored bias subsequent groups of ants exploring the same maze, which are then attracted to segments of increased pheromone concentration. Eventually, a set of optimal paths yield the best routes of domain exploitation for the colony. The intrinsic randomness of the process, in addition to the dissipation of pheromone concentration over time, ensure an appropriate exploration trade-off, where exploration is always encouraged but convergence is eventually achieved.

3.3 Algorithm implementation

In this paper, an ant corresponds to a combination of parameter values that results in a path, i.e., an alignment to be tested. We implemented an HDD ACO algorithm and tested it for two different design scenarios. The first one considers an alignment with fixed entry and exit points and a single straight segment in the central portion, with no

horizontal curvature. The plan view of such alignment is a straight line connecting the entry and exit points and remains unchanged by the algorithm. The profile view changes as a function of the input parameters. Figure 3, Case 1 shows two possible solutions generated by the algorithm in this scenario; the entry and exit points remain fixed for both solutions while the entry/exit angles and H vary, changing the length of the segments of the alignment with them.

The second scenario considers that the plan view of the central portion of the alignment is fixed and that its profile view can only change in elevation, while the location of the entry and exit points is flexible, as shown in Figure 3, Case 2. This scenario allows modeling alignments where the azimuth of the entry and exit tangents is different and/or the central portion must go around obstacles. The central portion can then include an arbitrary number of segments that can be either straight or curved. The elevation of the central segments is controlled by the variable H, used as the reference for the whole central portion. The entry and exit points of the alignment vary within acceptable ranges defined by the user.

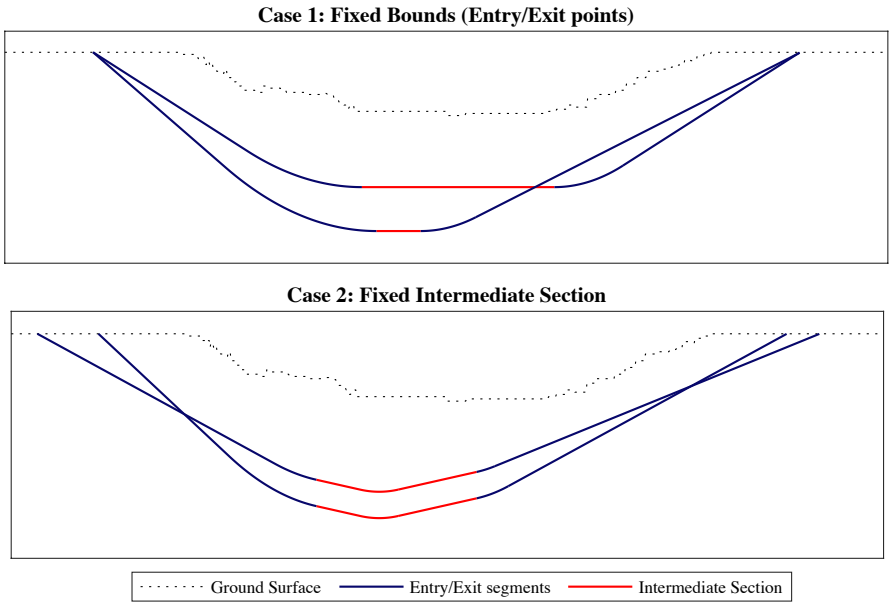

Figure 3. Implemented geometric scenarios. Each case shows an example of two different possible ACO solutions. Case 1 has a fixed location of entry/exit points with a variable intermediate straight segment. Case 2 shows an intermediate section configuration with a fixed geometry (curvature) but variable elevation and variable entry/exit points location.

The ACO algorithm for HDD design is implemented in two main steps. First, in the initialization of the algorithm (see section 3.4), the domain of exploration is defined. In our case, the intervals in which the design parameters range are set. Secondly, in the optimization step (see section 3.5), the knowledge of the domain is improved iteratively, therefore producing better solutions.

Before the initialization of the algorithm, the ranges of variation of the optimization variables are set and the size (n) of the solution ledger is fixed. Then, during the initialization step, n initial solutions are found from simple random combinations of the variables. Then the optimization algorithm runs a number (nG) of simulation batches, named generations. An ant is defined as a stochastic combination of the optimization variables (α, β and H); after an ant is constructed by the algorithm, it is evaluated. If the ant satisfies the geometric and mechanical constraints described in Section 2, and if

it yields a valid design, then the ant becomes a solution, and it is stored in the ledger by the algorithm. The process is stopped when nG generations have been simulated or when a convergence flag has been triggered. The convergence flag is usually set to stop when the difference between the output of two consecutive generations is below a set threshold. Algorithm 1 shows the outline of the implementation.

Algorithm 1: ACO-HDD Implementation

Initialization	1 - Set variable ranges
(Section 3.4)	2- Find initial n viable ants (randomly)
	While termination criterion is not satisfied **do:**
	1 - Update/Sort Solution Ledger
	2 – Find k viable ants:
Optimization	**While** less than k new solutions have been found
(Section 3.5)	**do:**
	Construct Ant
	Evaluate Geometry and Mechanical viability
	If Ant is successful, **then:** store as solution

3.4 Initialization

Step 1 – Variables range: The first stage of the initialization consists in finding valid ranges of variation of the optimization variables. To do so, a set of project specific parameters are needed: the profile of the ground surface elevation along the HDD path, the location and geometry of any obstacles that must be avoided by the algorithm, the characteristics of the drill equipment, which partially define the range of the entry and exit angles and the minimum segment length, and other project specific parameters including the radius of curvature, usually a function of the product pipe to be installed, and the minimum depth of cover. The elevation profile and the location of obstacles along the drill path control the maximum elevation of the alignment. Once this maximum H is found, the corresponding α_{max} and β_{min} angles necessary to reach that value of H are found geometrically and adjusted as necessary to fit in the initial user-

defined ranges. Conversely, the steepest angles α and β yield the lowest possible elevation of the alignment, therefore setting the minimum value of H.

Step 2 – Initial ants: After finding the valid ranges of variation for each one of the optimization variables, we find the initial n solutions (viable ants) that will start the algorithm. To do so, random combinations of parameters (ants) are tested, assuming that all the parameters follow a uniform probability distribution within their respective ranges. The process stops when n successful ants have been found, and their information, e.g. their values of H, α and β, and the resulting total length of the alignment stored on a ledger. This solution ledger is an archive that stores the colony's knowledge about the domain and that is updated during the optimization stage.

3.5 Optimization

The optimization algorithm repeats a subroutine over a loop until a convergence flag is reached or a fixed number of generations has been computed. Such subroutine is detailed below.

Step 1 – Update/Sort solution ledger: At every generation, the algorithm ranks the solutions in the ledger according to their quality or score. In our implementation, we define the score of a solution as the inverse of the total alignment length, therefore the best solution is the one that yields the shortest length while complying with all the geometric and mechanical constraints. Once the solutions are ranked from 1 to n, a weight (w_j) is associated to each solution j using a Gaussian function as shown in Eq 5.

$$w_j = \frac{1}{2qk\sqrt{2\pi}} \cdot e^{\frac{-(rank(j)-1)^2}{2q^2k^2}} \tag{5}$$

Where rank(j) is the rank of the solution j, and q is a user defined parameter of the algorithm. The probability of choosing a given solution (j) to create a new ant is:

$$p_j = \frac{w_j}{\sum_i^k w_i} \tag{6}$$

Values of q close to zero result in a highly skewed probability towards the higher-ranked solutions against lower-ranked solutions; conversely, very large values of q result in a uniform probability to choose any of the solutions in the ledger. The probability distribution of the solutions is also a function of n. Once the solutions ledger has been updated for the given generation, new ants are created and tested until a fixed number of (k) new solutions have been found.

Step 2 – Generation ants: Once the ledger has been updated, and with it the probability distribution of the current solutions in the ledger, we start a secondary loop which runs until we have found k new viable ants. The process of constructing a new ant (i.e., a combination of variable values) starts with the selection of a solution s from the ledger based on the discrete probability distribution described above. Then, a new value is independently assigned to each variable. A new value of variable (v) from solution (s) is sampled from a normal probability distribution with mean (μ) and standard deviation (σ) as shown in the probability density distribution in Eq. 7 below:

$$pdf(x) = \frac{1}{\sigma\sqrt{2\pi}} \cdot e^{\frac{-(x-\mu)^2}{2\mu^2}} \tag{7}$$

Where (μ) is taken as the value of variable v in the chosen solution s, and the standard deviation (σ). The standard deviation is a measure of the dispersion of the variable across the current solutions in the ledger; it is calculated as shown in Eq. 8, below:

$$\sigma = \frac{\varepsilon}{n-1} \cdot \sum_{i=1}^{n} |v_s - v_i| \tag{8}$$

The parameter epsilon (ε) is a user-defined parameter that affects the convergence speed of the algorithm; high values of epsilon result in high standard deviations, which slow down convergence and vice-versa. Similar to the parameter q, the choice of epsilon depends on the application and the desired runtime of the algorithm; fast convergence may result in unsatisfactory exploration of the domain.

Once an ant has been constructed, its viability is tested in reference to the geometric and mechanical constraints of the problem. In the first case, with fixed entry/exit points, the horizontal length of the entry and exit tangents and vertical curves is completely defined by the design parameters (α, β and H), and subsequently, the length of the central segment is fully determined. The alignment is geometrically acceptable if the length of each of the straight segments exceeds the minimum segment length and the minimum depth of cover is maintained along the alignment.

In the second case, the curvature and x and y coordinates of the intermediate segment is fixed, but the entry and exit points locations change as a function of the optimization parameters (α, β and H). Therefore, in addition to checking that the length of the segments is above the minimum, it is necessary to check that the entry and exit points fall within their allowable ranges (defined by the user). Figure 3 shows examples of drill paths for both cases.

Once it was verified that the alignment satisfies the geometric constraints of the problem, the mechanical stability of the borehole is checked for pilot drilling and pullback; the MAP (maximum allowable pressure before blowout is triggered) and MDP (minimum drilling pressure to induce fluid recirculation) are compared every 0.3m (1ft.). If there is a risk of blowout along the path (when MDP>MAP), the alignment is declared not acceptable; a relaxation of this rule is considered if the blowout location is located at shallow depths (less than 10ft / 3m from the ground surface) in the vicinity of the entry and exit points.

The mechanical validation requires calculating the stresses exerted on the product pipe as it is being pulled into the borehole. Similar to the blowout estimation, the pullback stresses are quantified every 0.3m including the contributions of tension and bending. Buckling is also checked. If the tested alignment (ant) is viable, it becomes a solution and is temporarily stored in the ledger.

After k new solutions have been found, the solution ledger has a total of (n+k) solutions, n from the previous step plus the newly generated solutions in the present generation. The (n+k) solutions are sorted according to their score, and the k solutions with the lowest scores discarded, therefore, at the end of each generation, there are exactly n solutions in the ledger.

This procedure is repeated for each generation, until the convergence criterion has been met or after a fixed number of generations have been computed. At the end of the optimization stage, the solution ledger has the best n viable combinations of parameters found by the algorithm.

4. Algorithm evaluation

In order to assess the performance of the algorithm, we study two design scenarios: one in which the entry and exit points are fixed (scenario 1) and one in which the curvature of the central portion of the alignment is fixed (scenario 2). For each scenario, we present two tests: one using synthetic data, for which the optimal solution is known, and one using real data from actual constructed projects, designed without ACO. Project datasets were provided by Haley Aldrich Inc.

In the simulations with synthetic data, the goal is to study the trends of the solutions returned by the algorithm over large domains and generation numbers, therefore we set the solution ledger size (n) to 100 and the number of generations (nG) to 50. Conversely, for the cases with real data, where the ranges of values for the geometric parameters are more restricted in nature, we set n equal to 25 and nG equal to 30.

For every instance tested, 5 new solutions are found by the algorithm at every optimization generation (i.e., k=5). In order to show the asymptotic behavior of the solutions, no convergence criterion was set, i.e. the nG generations of solutions were calculated. For all the instances, the parameter q was set to 0.45, resulting in probabilities of 9% and 1% to choose the 1st (best) and 25th solutions in the ledger,

respectively. The parameter epsilon (ε), which controls the standard deviation around the design parameters, was set to 1.25.

4.1 Scenario 1: Fixed Entry/Exit HDD points

The drilling path in the first scenario, when the entry and exit points of the alignment are fixed, is modelled as an alignment composed by 5 segments, including 3 straight segments (entry and exit tangents, plus the central segment), and 2 vertical curves, one at each side of the central segment (see Figure 3). Once the entry and exit points are assigned, the configuration of the vertical curves and the subsequent depth of the drill path are to be designed and optimized.

4.1.1 Proof of concept: synthetic data

We consider a simple horizontal profile with a constant elevation (100 ft), the entry and exit points are set at stations 0 and 2000 respectively. The range of the entry and exit angles are fixed between 10 and 20 degrees and the radius of curvature of the vertical projection of the curve is set to 1000 ft. We released the mechanical constraints (borehole stability and pipe integrity) in order to find the shortest and longest possible paths of the alignment. Then, the goal of the proof of concept simulations is to evaluate if the algorithm can yield close-to-optimal geometric solutions.

The minimum possible length of the drill path corresponds to an alignment with the shortest possible entry and exit tangents (minimum value set at 50 ft) and the smallest possible magnitude of their angles (10 degrees). Conversely, the longest drill path corresponds to entry/exit tangents with the maximum magnitude of their angles (20 degrees) and the minimum length of the central segment (50 ft). Such alignments are shown in Figure 4.

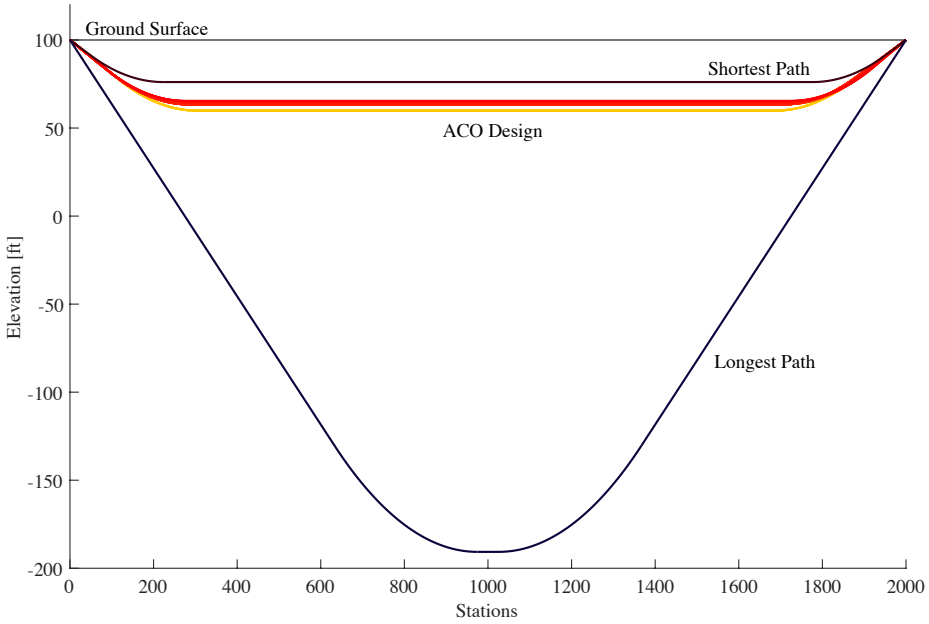

Figure 4. Shortest and Longest possible alignments and obtained ACO solutions. Scenario 1: fixed entry/exit points.

475

In order to show the progressive variation of the variable ranges inside the algorithm, Figure 5 shows the evolution of the distribution of the entry angles of the solutions in the ledger as a function of the calculation generations.

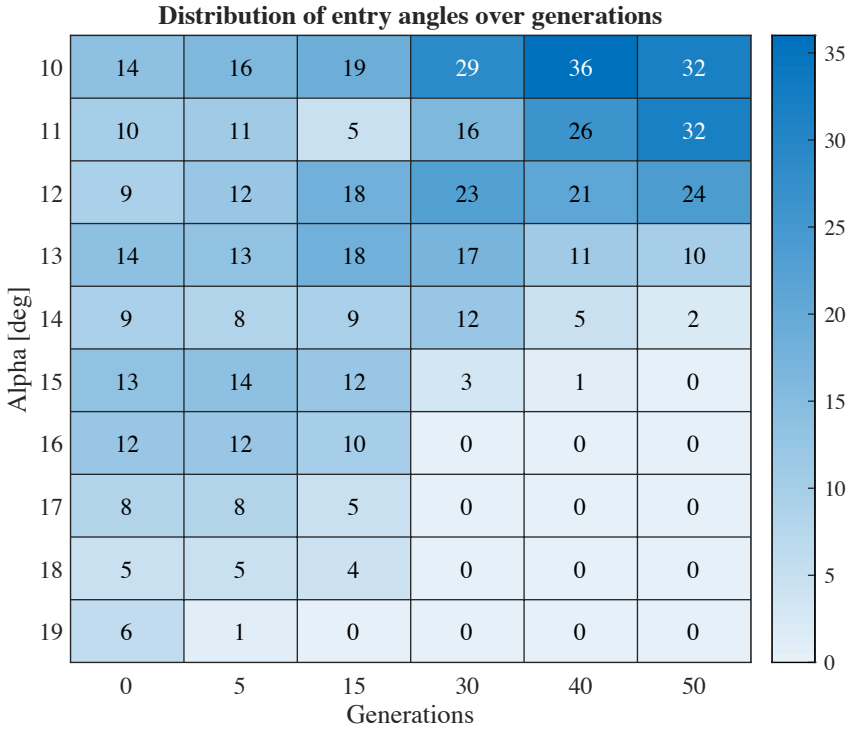

Figure 5. Distribution of entry angle over generations. Scenario 1: fixed entry/exit points. Values and color intensity correspond to the percentage of solutions in the corresponding bin, e.g. the sum of values in each column equals to 100.

The entry angles at initialization (generation 0) follow a relatively homogeneous distribution, after which, the distribution progressively narrows down to values closer to 10 degrees, the optimal solution. Lastly, we compare the evolution of the drill length of the ACO solutions against its maximum and minimum values, as shown in Figure 6.

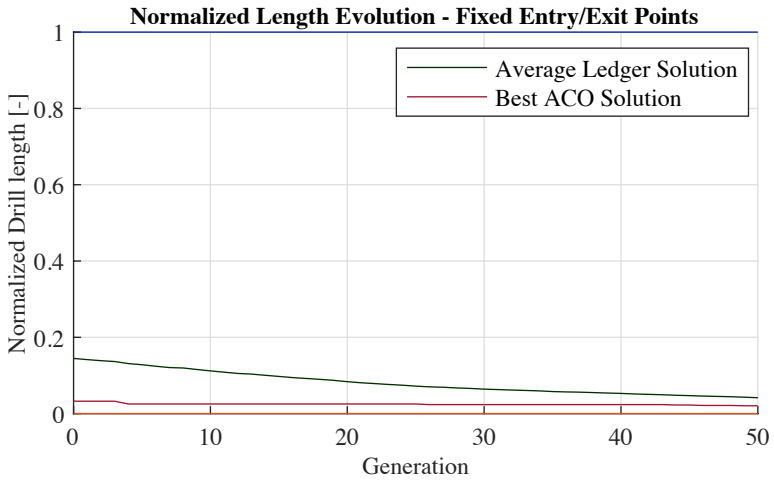

Figure 6. Evolution of ACO drill length over generations – Scenario 1: fixed entry/exit points. Normalized drill path length: a value of 1 (respectively 0) means that the drill path length equals the maximum value (respectively, minimum value), at entry/exit angles of 20° (respectively, 10°).

Obtained results show a progressive improvement of the best solution found by ACO resulting in a final drill length that its only 0.1% longer than the global minimum. In the same way, the average length of the solutions in the ledger decreases monotonically, indicating all the solutions in the ledger improve over generations.

4.1.2 Application to real project data

The project considered as an example is a drill passing below a traffic crossing, constructed to connect two sections of an underground power line. The rest of the alignment is built using conventional open trench techniques. The HDD drill hosts a FPVC casing pipe (10 in. in diameter), through which a bundle of power lines will be installed. The total (fixed) plan length of the drill is 2,250 ft (685.8 m). Due to the available equipment and space constraints at the exit site, including pullback area and existing overhead utilities, the range of the entry and exit angles was fixed between 10 and 16 degrees. A minimum depth of cover of 15 ft (4.57 m) and a vertical curve radius of 1,000 ft (304.8m) were adopted for the alignment.

The properties and characteristics of the product pipe to be installed as well as the equipment and drilling mud are fixed at the first step of the design. Therefore, the optimization step focuses on finding the geometrical configuration of the alignment in terms of the entry/exit angles (α, β) and the bottom elevation of the path (H). Figure 7 shows the actual drill path originally designed for the project and the region showing the evolution of the ACO optimized design over the generations (going from lighter to darker colors).

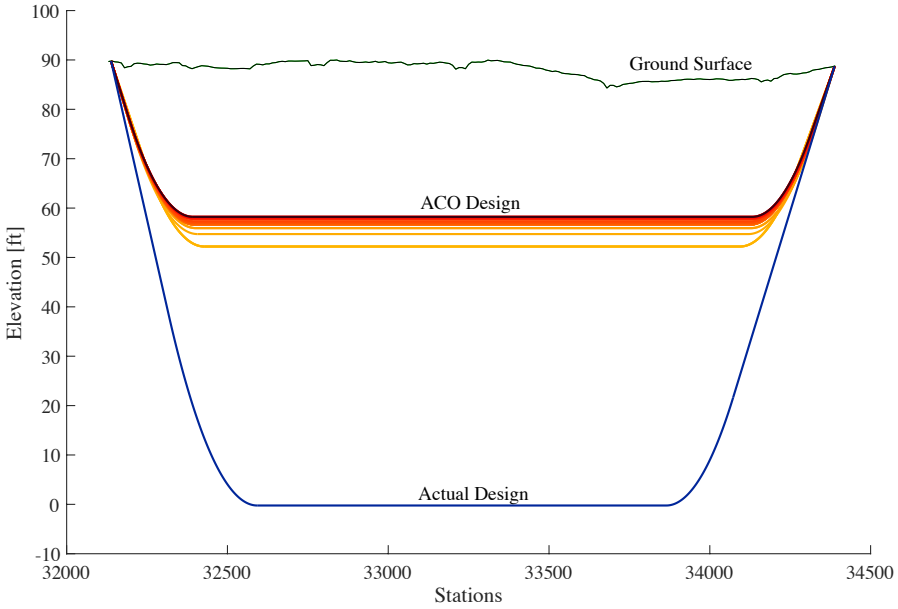

Figure 7. Actual and ACO drill path designs. Project in scenario 1: road crossing with fixed entry/exit points. Color intensity on the ACO design illustrates the different generations, going from lighter to darker colors.

Table 1 compares the total drill path length and the design parameters found by ACO with the actual design (AD) of the project.

Table 1. Scenario 1, summary of design parameters, actual design versus ACO path.

Case	*Drill Length [ft]*	*Bottom Elevation [ft]*	*Entry Angle [deg]*	*Exit Angle [deg]*
AD	2269.45	-0.23	-16	12
ACO	2254.73	57.82	-11.74	10.76

Obtained results show that even though the actual and the optimized drill paths are considerably different from each other, especially in terms of bottom elevation, the difference in drill path length is relatively small (under 15ft / 4.76m). This result shows that due to the fixed entry and exit points, this project offers little room for minimization of the drill path length.

In order to analyze the performance of the algorithm over the optimization generations, Figure 8 shows the evolution of the minimum drill path calculated by the algorithm against the actual drill path originally designed for the project. The geometric minimum corresponds to the shortest possible drill path to connect the entry and exit points and is shown only as a lower bound for reference since it is not a mechanically viable alignment.

In order to capture the distribution of the drill length of the solutions in the ledger, we study the evolution of the interquartile range (IQR), which corresponds to the difference between the values of the 3rd and 1st quartiles of the data, normalized by the geometric minimum bound. Large IQR values indicate that the algorithm has not converged yet, since significantly different drill lengths in the ledger imply a large variability of the design parameters being optimized. Similarly, the Mean-min difference is another measure of dispersion, this time quantifying the difference between the average and the minimum drill path lengths among the ledger at a given generation; large values suggest that further refinement of the solution domain is possible. The behavior of the dispersion and variability of the solutions in the ledger is a better indicator of convergence than the evolution of the best design (minimum drill length) alone since it captures the statistically representative state of the algorithm evolution, not a single solution.

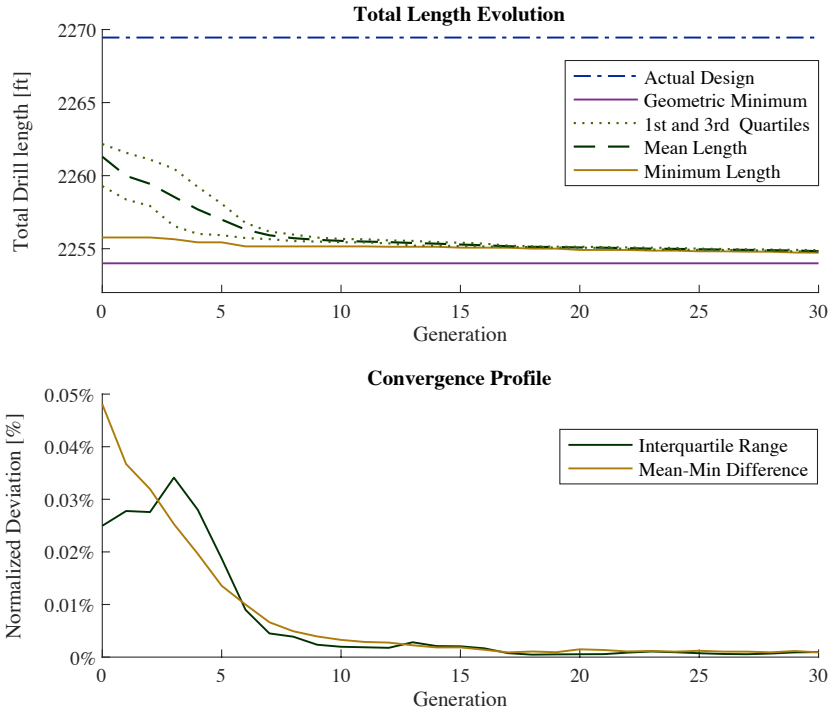

Figure 8. Drill path length evolution and convergence. Project in scenario 1: traffic crossing with fixed entry/exit points. Internal dispersion between the solution ledger and minimum drill path length reduce and stabilize after 11 optimization generations.

Figure 8 shows that the minimum drill path length found by ACO stabilizes after 11 generations, remaining relatively constant afterwards; due to the small room for minimization of this specific example, the obtained reduction in drill length over generations is about 5 ft (1.5m). The convergence profile shows low dispersion among the solutions in the ledger starting at the first generation. The dispersion is further reduced, to reach a stable optimized path with low dispersion.

The obtained optimized drill path is shorter than the originally designed path, while exhibiting a consistent convergence profile, showing the capability of the algorithm to automate the design process and reach convergence and minimization of the drill path even under highly restricted domains. Results from Figure 9, which illustrates the

evolution of the best combination of design parameters, such that they yield the minimum drill path length, show relatively constant values of entry and exit angles (α, β), while the bottom path elevation of the drill path (controlled by H) significantly changes over generations, even after the total drill path appears to stabilize.

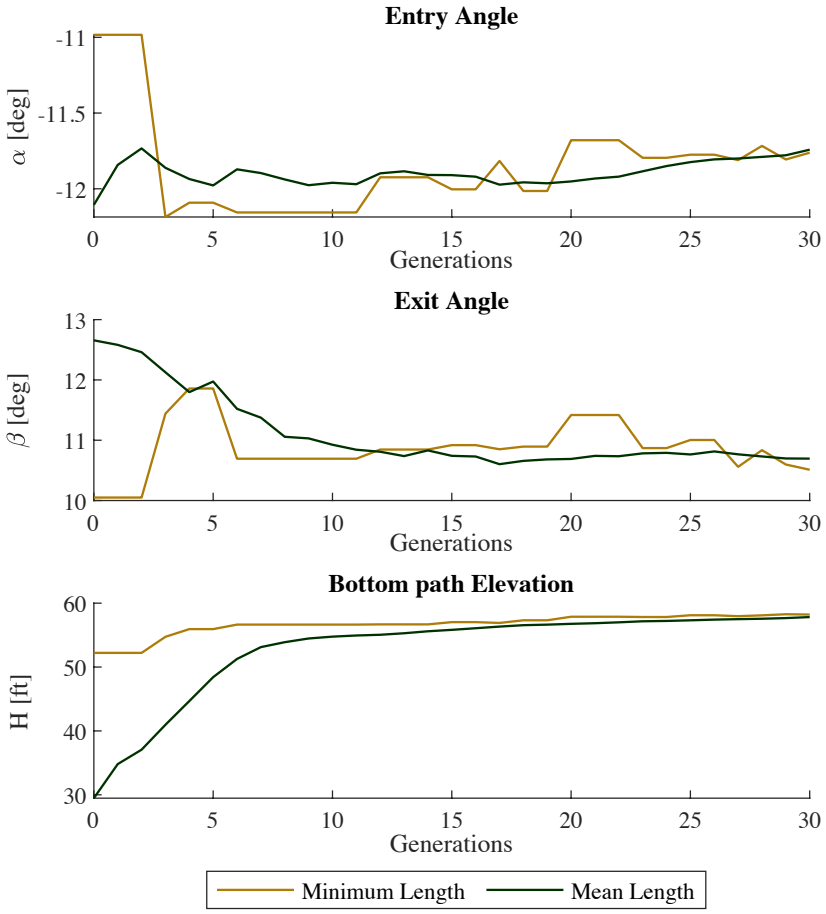

Figure 9. Evolution of optimized design parameters. Project in scenario 1: traffic crossing with fixed entry/exit points. Results show large variations of H while α, β show a small range of fluctuation.

4.2 Scenario 2: Constrained geometry of central segments

Here, the location of the entry and exit points can be adjusted within a certain interval. This design scenario is particularly useful when considering the existence of physical obstacles that the HDD alignment must avoid, or designs where the entry and exit azimuth of the alignment are different, in which case, horizontal or compound curves are necessary, and oftentimes located in the central region. Constraints on the entry and exit points depend on the accessibility conditions on site and are transferred to the algorithm in the form of two intervals for the allowable locations of the entry and exit points.

4.2.1 Proof of concept: synthetic data

We consider the same surface profile as the one described in Subsection 4.1.1 and an alignment with a single, horizontal segment in the intermediate region spanning from station 750 to 1250 (500 ft in length). The range of the entry and exit angles was fixed between 10 and 20 degrees and the radius of the vertical curve was set to 1000 ft. The entry/exit points of the drill can be placed within 375 ft from the start/end of the alignment respectively. Once again, we released the mechanical constraints (borehole stability and pipe integrity) and compared the results obtained by the algorithm to the global minimum and maximum drill path lengths. The shortest and longest drilling alignments, in addition to the best alignment obtained by the ACO algorithm are shown in Figure 10.

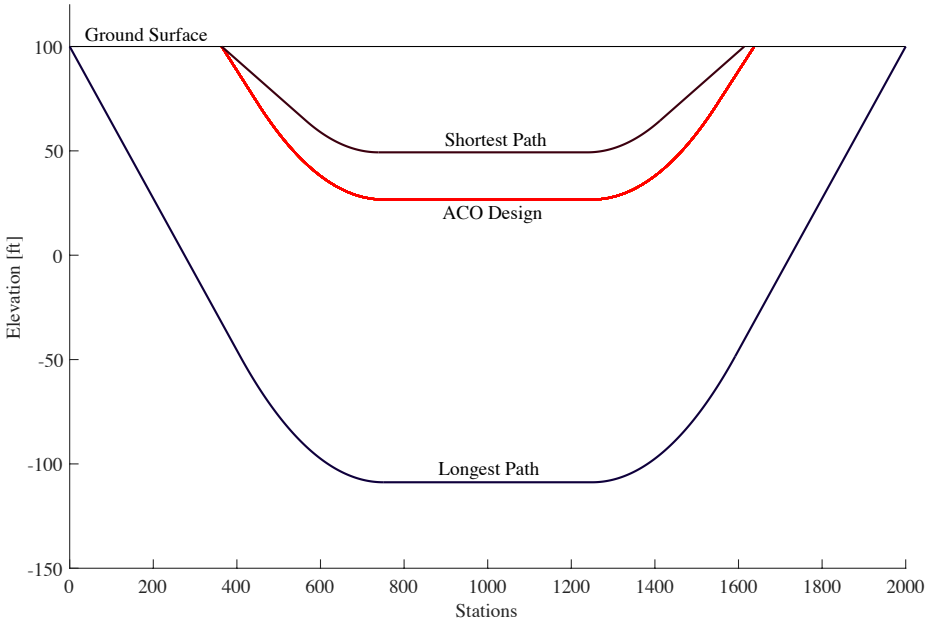

Figure 10. Shortest and Longest possible alignments and obtained ACO solutions. Scenario 2: Constrained geometry of the central segment.

Next, we show the evolution of the distribution of the vertical angle of the entry segment along the 50 calculation generations. The results are shown in Figure 11.

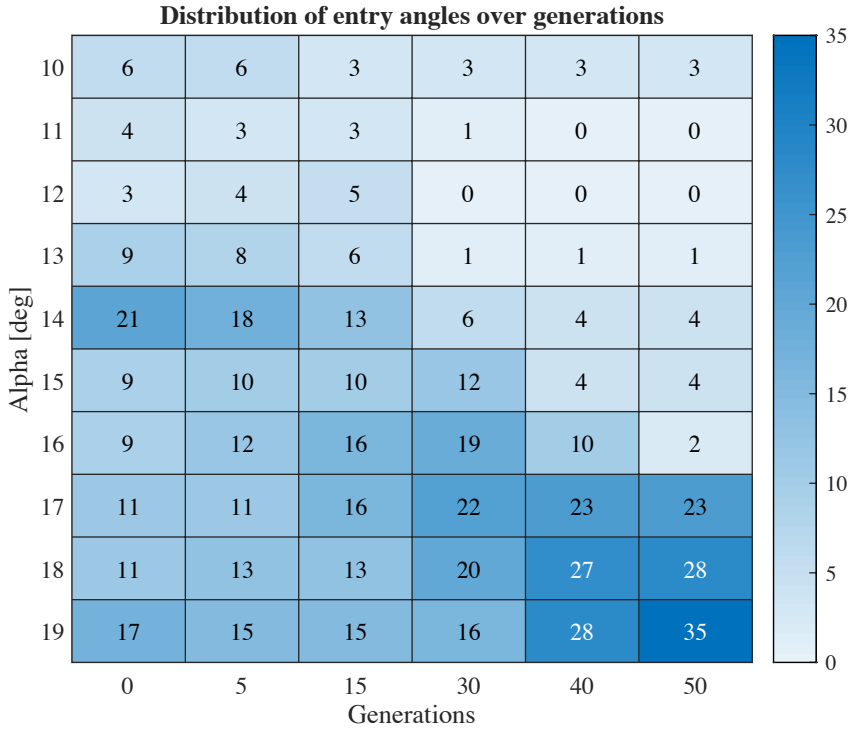

Figure 11. Distribution of entry angle over generations. Scenario 2: constrained geometry of the central segment. Values and color intensity correspond to the percentage of solutions in the corresponding bin, e.g. the cum of values in each column equals to 100.

Figure 11 shows a relatively uniform distribution of values at initialization, which shifts into a narrow distribution at later generations, suggesting the algorithm has centered around a small range of values. Then, we compare the total length of the solutions found by the algorithm over the generations to the minimum and maximum lengths; the best and average drill path lengths are shown in Figure 12.

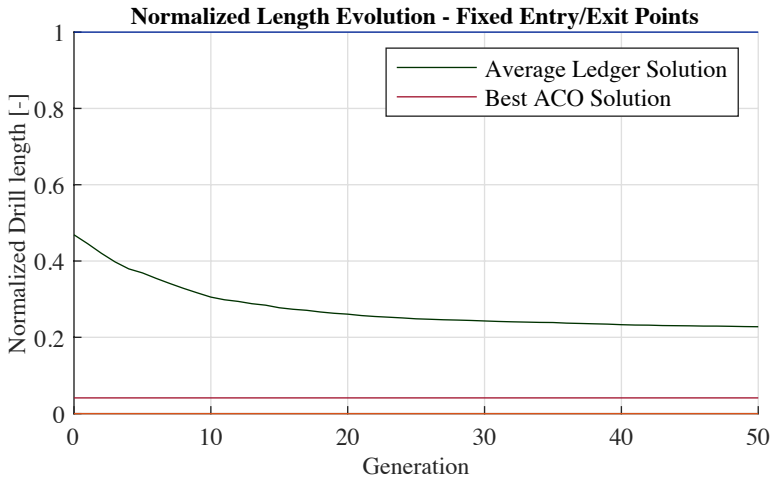

Figure 12. Evolution of ACO drill length over generations – Scenario 2: constrained geometry of the central segment. Normalized drill path length: a value of 1 (respectively 0) means that the drill path length equals the maximum value (respectively, minimum value), at entry/exit angles of 20° (respectively, 10°).

Figure 12 shows that the average length of the solutions in the ledger decreases as the number of generations increases. However, one of the initial random solutions generated proved to be the best, even after running the different generations, such solution had a total drill length that is only 2.65% longer than the optimal minimum. It is worth noting that this second scenario, with a flexible location of the entry/exit points, yields a significantly higher variability of the solution domain compared to scenario 1, with fixed entry/exit points.

4.2.2 Application to real project data

The project taken as an example here is a drill passing below a shipping channel in an industrial port area, constructed to connect a power line from an electric substation to the rest of the underground alignment. The rest of the project is built using conventional open trench techniques parallel to an existing road. The presence of several foundations from surrounding structures around the shipping canal constrains the design of the drill alignment. Therefore, a fixed plane central region of the alignment includes a compound helix curve with an 1800 ft (568.4 m) radius, a vertical slope of 0.7 degrees and a 16 degrees horizontal angle. Two adjacent straight segments with the same slope and lengths of 23.9 ft (7.3 m) and 13.48 ft (4.1 m) at the entry and exits

point sides complete the central region, Figure 2 shows the configuration of such an alignment in plan and profile views.

Besides the three segments described in the central region of the alignment, four other segments complement the drill path, two vertical curves and two straight segments, one of each at each side of the central region. The HDD drill hosts a steel casing pipe (34 in in diameter) through which a bundle of power lines will be installed. The range of the entry and exit angles was fixed between 8 and 14 degrees. A minimum depth of cover of 15ft (4.57 m) was determined for the design, and the radius of the entry and exit vertical curves was fixed to 1,800 ft (568.4 m), the same as the horizontal radius of the helix curve.

In order to test the effect of the constraint imposed on the location of the entry and exit points, two different instances of the algorithm were tested, one with a 50 ft. viability range for both the entry and exit points (ACO – 50 ft.), and the other with a 150 ft. range for both the entry and exit points (ACO – 150 ft,). Table 2 shows the allowable limits for the location of the entry and exit points for each instance.

Table 2. Scenario 2: Entry and exit drill points viability ranges.

Case	*Entry Area*			*Exit Area*		
	Min	*Max*	*Actual*	*Min*	*Max*	*Actual*
AD	-	-	50	-	-	1942.7
ACO – 50ft	50	100	99.8	1900	1950	1904.8
ACO – 150ft	50	200	184.0	1800	1950	1802.3

Figure 13 shows the actual drill path originally designed for the project, and the evolution of the ACO optimized design over the generations, for each of the two instances. Table 3 compares the total drill path length and the design parameters of the actual design (AD) with those of each of the two ACO instances.

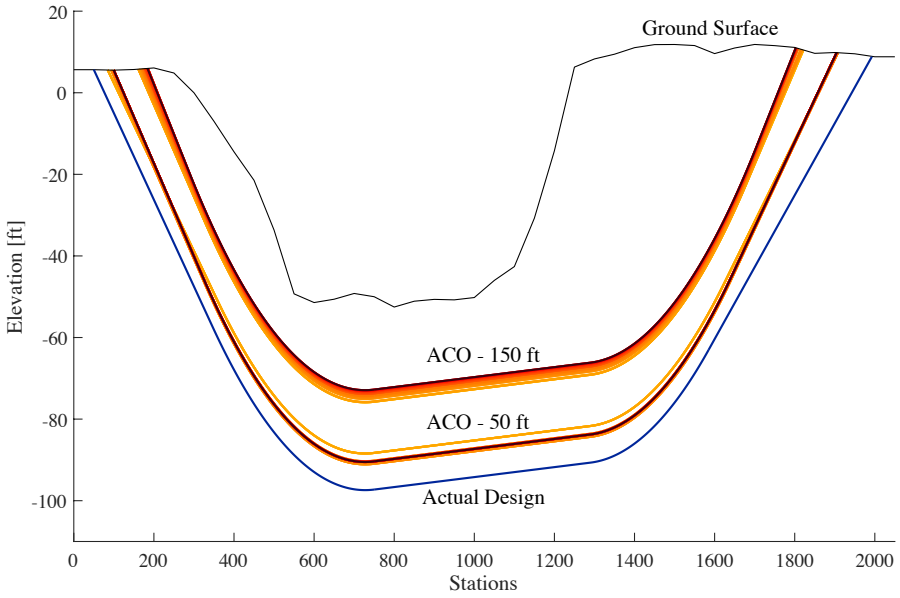

Figure 13. Actual and ACO drill path designs. Project in Scenario 2: river crossing with fixed central region design and flexible entry/exit points. Results shown for two ACO instances with different flexibility ranges. Color intensity on the ACO designs corresponds to subsequent generations, going from lighter to darker colors.

Table 3. Scenario 2, summary of design parameters, actual design (AD) versus ACO instances.

Case	*Plane Length [ft]*	*Drill Length [ft]*	*Bottom Elevation [ft]*	*Entry Angle [deg]*	*Exit Angle [deg]*
AD	1892.7	1960	-97.27	-12	10
ACO – 50ft	1805	1822.8	-90.27	-12.78	11.75
ACO – 150ft	1618.3	1634.3	-72.89	-13.75	13.76

Obtained optimization results show that setting the drill path length as the optimization objective results in the minimization of the plane length as well, by selecting entry and exit locations as close as possible to the boundaries of the viable ranges. Not surprisingly, a higher flexibility results in reduced drill path length and as the variability range increases, the optimized design parameters increasingly differ from the actual

design (in this case, steeper entry/exit tangents and a significantly shallower drill are obtained by ACO design).

Figure 14 shows the distribution of the drill path length stored in the solutions ledger over the generations. In a similar way to Scenario 1, the evolution of the minimum (best) length, mean and the 1st and 3rd quartile values are shown over the 30 optimization generations. Given that design ranges for the entry/exit points locations are different for the different instances, their results are not directly comparable to each other, and are meant to illustrate the effect of different design considerations on the performance of the algorithm.

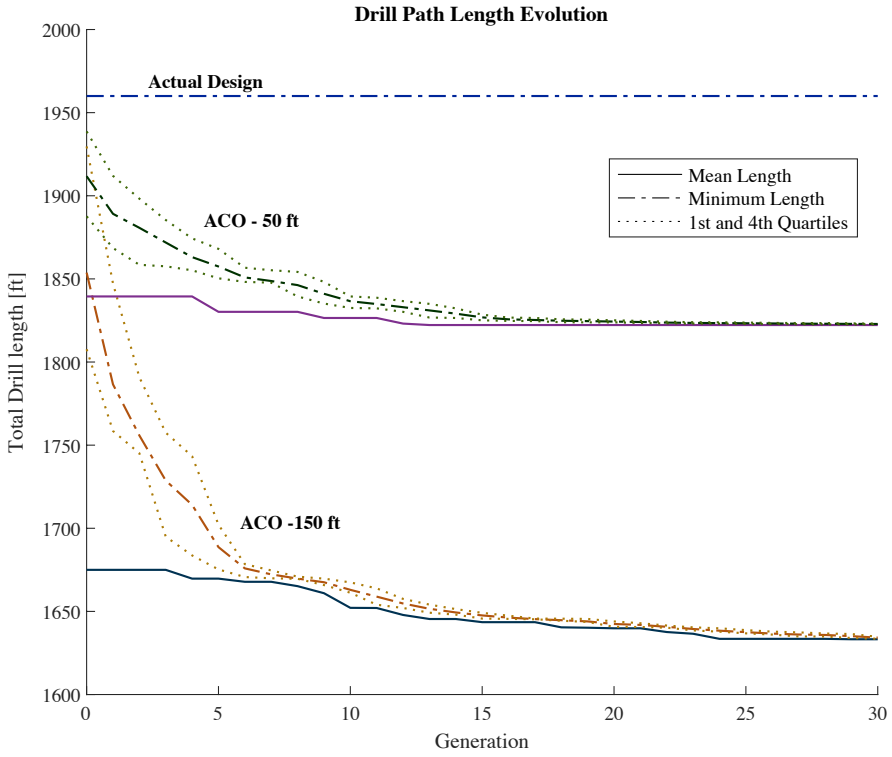

Figure 14. Drill path length evolution. Project in Scenario 2: river crossing with two different instances with different entry/exit point location flexibility ranges. Increased flexibility results in shorter paths and increased room for parameter optimization, at the expense of slower convergence.

Results from Figure 14 show the influence of the location of the entry/exit points in the drill path length. As expected, instances with shorter allowable plane lengths yield shorter drill path lengths. Furthermore, the broader search domain created by the increased flexibility of the entry and exit points results in greater minimization of the initial mean drill path length over generations. In terms of convergence, the minimum optimized drill path length stabilized at generation 12 for ACO -50 ft, while it stabilized on generation 23 for ACO – 150 ft. Figure 15 shows the evolution of the dispersion measures defined in section 4.1 (IQR and mean-min difference) but this time normalized by the minimum drill length for each instance.

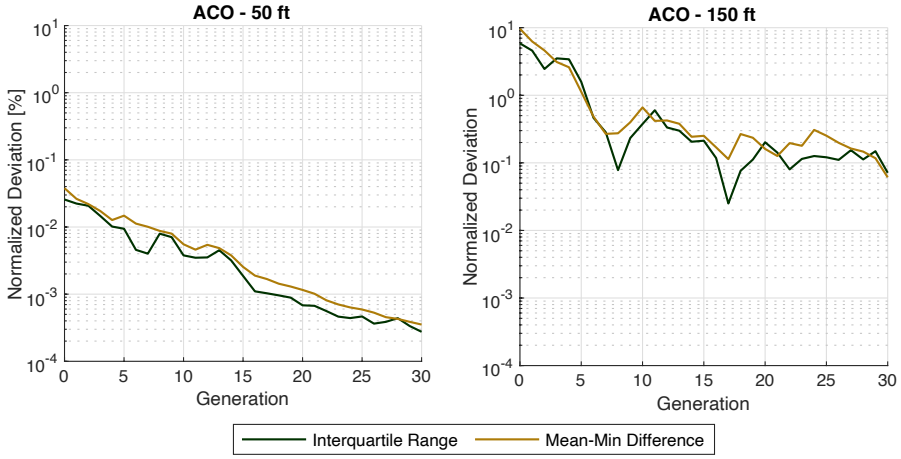

Figure 15. Evolution of path length dispersion indexes. Project in Scenario 2: river crossing with two different instances with different entry/exit point location flexibility ranges. Increased flexibility significantly increases the internal solution ledger deviation.

Results from the convergence profile in Figure 15 show a significantly larger dispersion among the ledger solutions of ACO – 150 ft. compared to ACO – 50 ft. In both instances though, the dispersion consistently decreases over the generations. This fact suggests that as the flexibility of the domain increases, the potential of minimization increases, enlarging the search domain and potentially improving the optimized solution; but this is at the expense of slower convergence.

This observation is supported by the evolution of the optimal design parameters, as shown in Figure 16. The variation of each parameter from the first generation to the last is considerably larger for the more flexible instance (ACO -150 ft) compared to the more restricted instance (ACO-50 ft). The values of the optimal design parameters seem to stabilize after the first 10 generations for both instances, showing the point at which the exploration of different paths stops, and the algorithm starts converging.

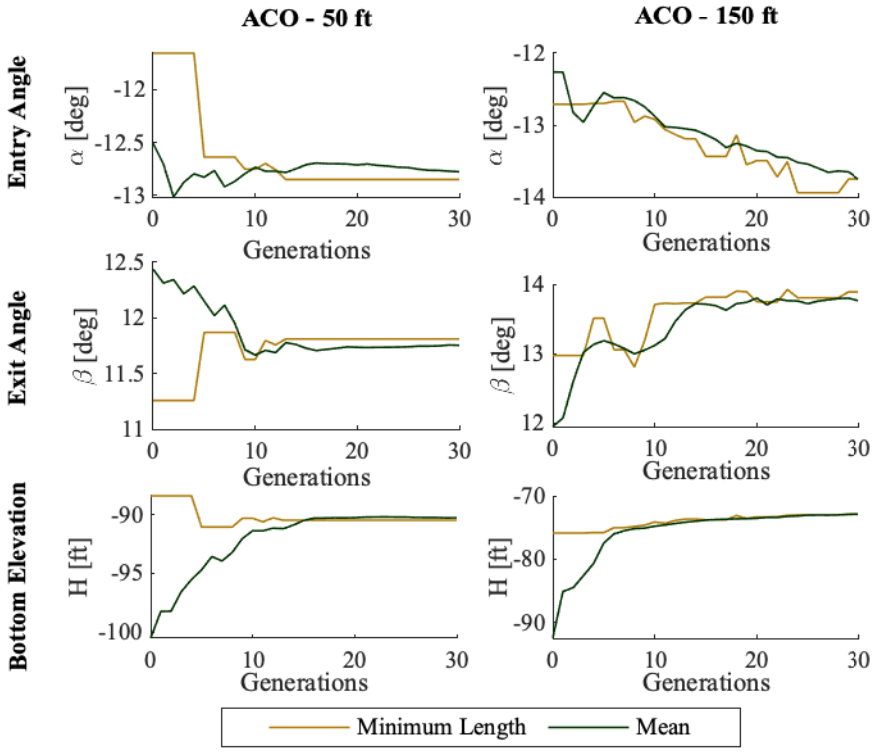

Figure 16. Evolution of optimized design parameters. Project in Scenario 2: river crossing with two different instances with different entry/exit point location flexibility ranges. Increased flexibility results in broader fluctuation ranges for optimization parameters.

5. Conclusions

Horizontal Directional Drilling (HDD) is gaining increasing interest in the engineering practice because of its relatively low cost, environmental impact, land use

and project timeline. Despite its efficiency, HDD relies on empirical and iterative design. To aid routine design procedures, we applied an Ant Colony Optimization (ACO) algorithm to automatically minimize the drill path length under given geometrical constraints (such as the underground path, that might have to fit between obstacles, or the entry and exit points, which have to be accessible on site), and mechanical constraints (to avoid pipe failure or instability).

Results show the potential of heuristic algorithms like the ACO implementation to automate the design process of HDD alignments and leverage the need of manual iterations from the design engineer. In terms of minimization of the drill path length, the algorithm consistently minimized the drill length over the computation generations, showing a more pronounced decrease in open domains where the design parameters have high flexibility.

The algorithm reached an asymptotic behavior in all the tested instances, showing that broader (less restricted) domains translate into more extensive exploration steps and therefore need more computation generations to reach an asymptotic behavior and convergence. In terms of running time, the algorithm is affected not only by the convergence parameters but also by the ease of finding new valid solutions, which depends on the geometric configuration and input parameters of the design. Nevertheless, the optimization algorithm does not incur in extensive computation times, being always under 15 minutes of run time using a serial implementation on a 2.40 GHz machine (Intel i5-6300U) for each of the instances tested.

A natural extension of the present work will be to release the constraint that imposes that the optimization of the path occurs along a fixed alignment in plane view, which must be decided *a priori* by the design engineer. Future implementations could include a more comprehensive search domain, which instead of being limited to a 2D (fixed) geotechnical profile, could include a 3D domain to find the best path between two allowable entry and exit areas. Nonetheless, this extension of the algorithm requires a

significantly more extensive knowledge of the topographic and geotechnical characteristics of the 3D construction domain.

Lastly, it is important to highlight that the accuracy and viability of the algorithm is based on the set of constraints and variables on which the algorithm is built on, therefore the current implementation does not intend to replace the judgment of a trained engineer who must validate the input parameters and results obtained from the algorithm.

Acknowledgements

The authors acknowledge and thank Haley Aldrich, Inc. for providing and assisting with the data used in the present study.

This research did not receive any specific grant from funding agencies in the public, commercial, or not-for-profit sectors.

References

1. Sarireh M, Najafi M, Slavin L. Usage and Applications of Horizontal Directional Drilling. In: ICPTT 2012. Reston, VA: American Society of Civil Engineers; 2012. p. 1835–47.
2. Allouche EN, Ariaratnam ST, Lueke JS. Horizontal Directional Drilling: Profile of an Emerging Industry. J Constr Eng Manag. 2000;126(1):68–76.
3. Bennett D, Ariaratnam ST. Horizontal Directional Drilling: Good Practices Guidelines. 4th ed. North American Society for Trenchless Technology; 2017.
4. Yan X, Ariaratnam ST, Dong S, Zeng C. Horizontal directional drilling: State-of-the-art review of theory and applications. Tunn Undergr Sp Technol. 2018 Feb 1;72:162–73.
5. Xia HW, Moore ID. Estimation of maximum mud pressure in purely cohesive material during directional drilling. Geomech Geoengin [Internet]. 2006 Mar 22 [cited 2019 Sep 13];1(1):3–11. Available from:

http://www.tandfonline.com/doi/abs/10.1080/17486020600604024

6. Shu B, Zhang S, Liang M. Estimation of the maximum allowable drilling mud pressure for a horizontal directional drilling borehole in fractured rock mass. Tunn Undergr Sp Technol [Internet]. 2018 Feb 1 [cited 2019 Sep 13];72:64–72. Available from: https://www.sciencedirect.com/science/article/pii/S0886779817303760

7. Rabiei M, Yi Y, Bayat A, Cheng R. General method for pullback force estimation for polyethylene pipes in horizontal directional drilling. J Pipeline Syst Eng Pract. 2016 Aug 1;7(3).

8. Rostami A, Yi Y, Bayat A. Estimation of maximum annular pressure during HDD in noncohesive soils. Int J Geomech [Internet]. 2017 [cited 2019 Sep 13];17(4). Available from: https://ascelibrary.org/doi/pdf/10.1061/%28ASCE%29GM.1943-5622.0000801

9. Kennedy M, Skinner G, Moore I. Elastic calculations of limiting mud pressures to control hydrofracturing during HDD. In: Proceedings North American Society for Trenchless Technology, No-Dig 2004 New Orleans, Louisiana, March 22-24 [Internet]. 2004 [cited 2019 Sep 13]. p. 1–11. Available from: https://pdfs.semanticscholar.org/92e4/c6656e0c05670297a437af00747952dab0e2.pdf

10. Duyvestyn G. COMPARISON OF PREDICTED AND OBSERVED HDD INSTALLATION LOADS FOR VARIOUS CALCULATION METHODS. In: No-Dig Conf. 2009.

11. Baumert ME, Allouche EN, Moore ID. Drilling Fluid Considerations in Design of Engineered Horizontal Directional Drilling Installations. Int J Geomech [Internet]. 2005 Dec [cited 2019 Sep 13];5(4):339–49. Available from: http://ascelibrary.org/doi/10.1061/%28ASCE%291532-3641%282005%295%3A4%28339%29

12. Keulen B. Maximum allowable pressures during horizontal directional drillings focused on sands [Internet]. 2001 [cited 2019 Sep 13]. Available from: https://repository.tudelft.nl/islandora/object/uuid:ad91dad8-b958-481b-82d8-

c7395d1a3874

13. Huey DP, Hair JD, McLeod KB. Installation loading and stress analysis involved with pipelines installed by horizontal directional drilling. In North American Society for Trenchless Technology, Chicago, IL (United States); 1996.

14. American Society for Testing and Materials. F1962-11 Standard Guide for Use of Maxi-Horizontal Directional Drilling for Placement of Polyethylene Pipe or Conduit Under Obstacles, Including river crossings. 2011 [cited 2019 Sep 13];04:1–18. Available from: www.astm.org.

15. Holway DA, Case TJ. Mechanisms of dispersed central-place foraging in polydomous colonies of the Argentine ant. Anim Behav. 2000;59(2):433–41.

16. Kakas AC, Cohn D, Dasgupta S, Barto AG, Carpenter GA, Grossberg S, et al. Ant Colony Optimization. In: Encyclopedia of Machine Learning. Boston, MA: Springer US; 2011. p. 36–9.

17. Dorigo M, Di Caro G. Ant colony optimization: a new meta-heuristic. In: Proceedings of the 1999 Congress on Evolutionary Computation-CEC99 (Cat No 99TH8406). IEEE; 1999. p. 1470–7.

18. Dorigo M, Stützle T. Ant colony optimization: Overview and recent advances. In: International Series in Operations Research and Management Science. Springer New York LLC; 2019. p. 311–51.

19. Samà M, Pellegrini P, D'Ariano A, Rodriguez J, Pacciarelli D. Ant colony optimization for the real-time train routing selection problem. Transp Res Part B Methodol. 2016;85:89–108.

20. Yang Z, Yu B, Cheng C. A Parallel Ant Colony Algorithm for Bus Network Optimization. Comput Civ Infrastruct Eng. 2007;22(1):44–55.

21. Liao T, Socha K, De Oca MAM, Stutzle T, Dorigo M. Ant colony optimization for mixed-variable optimization problems. IEEE Trans Evol Comput. 2014;18(4):503–18.

22. Bottinelli A, Wilgenburg E van, Sumpter DJT, Latty T. Local cost minimization in ant transport networks: from small-scale data to large-scale trade-offs. J R Soc Interface. 2015;12(112):20150780.